# 10 - 16 μm Broad-band quantum well infrared photodetector

S. V. Bandara, S. D. Gunapala, J. K. Liu, E. M. Luong, J. M. Mumolo, W. Hong, D. K. Sengupta and M. J. McKelvey

Center for Space Microelectronics Technology
Jet Propulsion Laboratory
California Institute of Technology
Pasadena, CA 91109

## ABSTRACT

A broad-band infrared detector, sensitive over a 10- 16 μm spectral range, based on $GaAs/Al_xGa_{1-x}As$ quantum wells grown by molecular beam epitaxy, has been demonstrated. Wavelength broadening of $\Delta\lambda/\lambda_p \sim 42\%$ is observed to be about a 400 % increase compared to a typical bound-to-quasibound quantum well infrared photodetector (QWIP). In this device structure, which is different from typical QWIP device structures, two different gain mechanisms associated with photocurrent electrons and dark current electrons were observed and explained. Even with broader response, $D^* \sim 1 \times 10^{10}$ cm $\sqrt{Hz}$ /W at T = 55 K is comparable to regular QWIPs with similar cutoff wavelengths.

## 1. INTRODUCTION

Long wavelength infrared QWIP cameras developed at the Jet Propulsion Laboratory[1-3], in collaboration with Raytheon Systems, demonstrate the potential of $GaAs/Al_xGa_{1-x}As$ QWIP technology for highly sensitive, low power, low cost, and highly uniform large format FPA imaging systems. These cameras utilize FPAs as large as 640x486 based on optimized $GaAs/Al_xGa_{1-x}As$ multi-quantum-well structures (MQWs) coupled with random or two dimensional periodic grating reflectors. FPA uniformity better than 99.95% after two point correction has been reported[1-3]. Other advantages of GaAs/AlGaAs based QWIPs are higher yield, durability, radiation hardness, and no 1/f noise till 30 mHz.

The detection mechanism of QWIP involves photoexcitation of electrons between ground and first excited state subbands of multi-quantum wells which are artificially fabricated (MQWs) by placing thin layers of two different, high-bandgap semiconductor materials alternately[4,5]. The bandgap discontinuity of two materials creates quantized subbands in the potential wells associated with conduction bands or valence bands. The structure parameters are designed so that the photo excited carriers can escape from the potential wells and be collected as photocurrent. In addition to larger intersubband oscillator strength, these detectors afford greater flexibility than the usual extrinsically doped semiconductor IR detectors because the wavelength of the peak response and cutoff can be continuously tailored by varying layer thickness (well width) and barrier composition (barrier height) [4-7].

## 2. SPECTRAL BANDWIDTH

Unlike the responsivity spectrums of intrinsic infrared detectors, the responsivity spectrums of QWIPs are much narrower and sharper due to their resonance intersubband absorption.[4,5] The normalized responsivity spectra $R(\lambda)$ are given in Fig. 1, where we see that the *bound* and *quasibound* excited state QWIPs are much narrower $\Delta\lambda/\lambda \sim 10\%$ than the *continuum* QWIPs $\Delta\lambda/\lambda = 24$ %. This is due to the fact that, when the excited state is placed in the continuum band above the barrier, the energy width associated with the state becomes wide[5-7]. At low operating bias voltages, responsivity spectrum of bound-to-bound QWIPs show additional peaks due to resonance energy levels of potential barriers (See Figure 2). The absorption between ground state and barrier resonance levels are much smaller than that of the ground and first excited state. The escape probability of the photoexcited electrons at the bounded first excited state is much smaller under lower operating bias voltages. As the bias increases, the escape probability of the photoexcited electrons at the excited state (bounded to the well) also increases. Thus the peak

associated with the bound to excited transition becomes dominant in the spectrum. Also, due to the same reason, bound-to-continuum QWIPs do not show any responsivity peaks associated with barrier resonances.

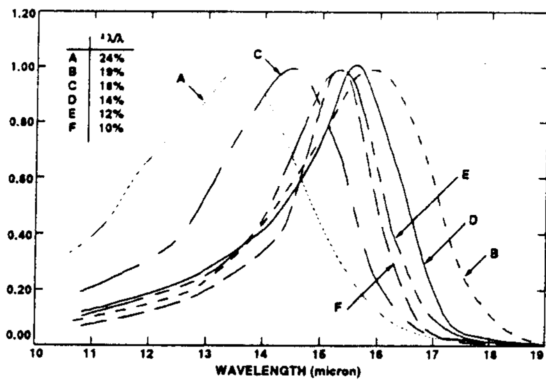


Fig. 1. Spectral band width variation of QWIPs with bound-to-bound, bound-to-quasibound and bound-to-continuum transitions.

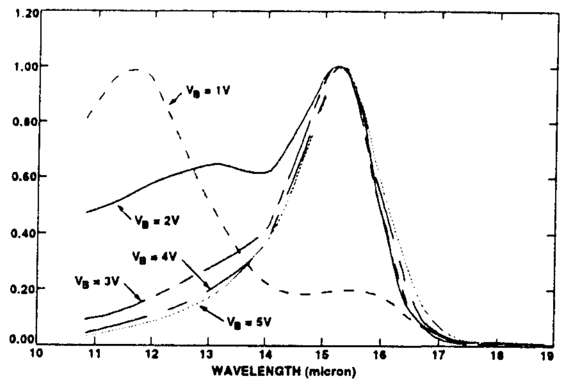


Fig. 2. Normalized spectral responsivity of a bound-to-bound QWIPs showing additional peak due to barrier resonance at lower bias voltages.

A broad-band MQW structure can be designed by repeating a unit of several quantum wells with slightly different parameters such as well width and barrier height. The positions of ground and excited states of the quantum well are determined by the quantum well width ($L_w$) and the barrier height, i.e. the Al mole fraction (x) of the barrier [4,5]. Since each single set of parameters for a bound-to-quasibound quantum well corresponds to a spectral band pass of about 1.5 μm, three different sets of values are sufficient to cover a 12-16 μm spectral region. As shown in Fig 1, the MQW structure consists of many periods of these three-quantum-well units separated by thick barriers. The device structure reported here involved 33 repeated layers of GaAs three-quantum-well units separated by $L_B$ ~ 575 A° thick $Al_xGa_{1-x}As$ barriers (See Fig 3). The well thickness of the quantum wells (see Fig. 3) of three-quantum-well units are designed to respond at peak wavelengths around 13, 14, and 15μm respectively. These wells are separated by $L_u$ ~ 75 A° thick $Al_xGa_{1-x}As$ barriers. The Al mole fraction (x) of barriers throughout the structure was chosen such that the $\lambda_p$ = 13 μm quantum well operates under bound-to-quasibound conditions. The excited state energy level broadening has been further enhanced due to the overlap of the wavefunctions associated with excited states of quantum wells separated by thin barriers. Energy band calculations based on a two band model show excited state energy levels spreading about 28 meV.

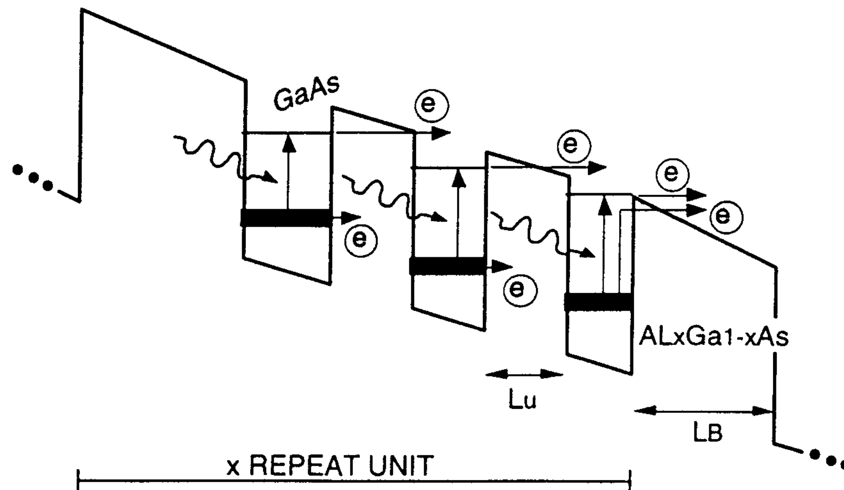


Fig. 3. Schematic diagram of the conduction band in broad-band QWIP in an externally applied electric field. The device structure consists of 33 repeated layers of three-quantum-well units separated by thick $Al_xGa_{1-x}As$ barriers. Also shown are the possible paths of dark current electrons and photocurrent electrons of the device under a bias.

The sample was grown on a semi-insulating GaAs substrate by molecular beam epitaxy. It consists of the device structure described above sandwiched between top and bottom contact layers. Transport carriers (electrons) were provided by doping all GaAs wells and contact layers with Si. In order to measure dark current-voltage curves, spectral responsivity and noise, 200 μm diameter mesas were fabricated using wet chemical etching and Au/Ge ohmic contacts were evaporated onto the top and bottom contact layers [4,5].

## 3. EXPERIMENTAL RESULTS

The responsivity spectra of these detectors were measured using a 1000 K blackbody source and a grating monochromator. The detectors were back illuminated through a 45° polished facet [4,5] to obtain normalized responsivity spectra at different bias voltages. Then the absolute spectral responsivities were obtained by measuring total photocurrent from a calibrated black-body source. In Fig. 4, responsivity curve at $V_B$ = -3 V bias voltage shows broadening of the spectral response up to $\Delta\lambda \sim 5.5$ μm, i.e. the full width at half maximum from 10.5 - 16μm. This broadening $\Delta\lambda/\lambda_p \sim 42$ % is about a 400 % increase compared to a typical bound-to-quasibound QWIP [1,8].

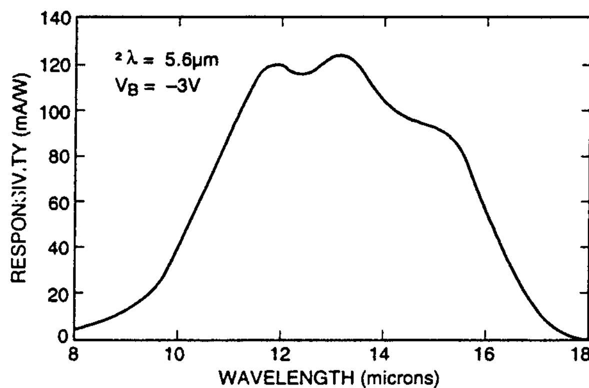


Fig. 4. Experimental measurements of the Responsivity spectrum of broad-band QWIP measured at the bias voltage VB = - 4 V.

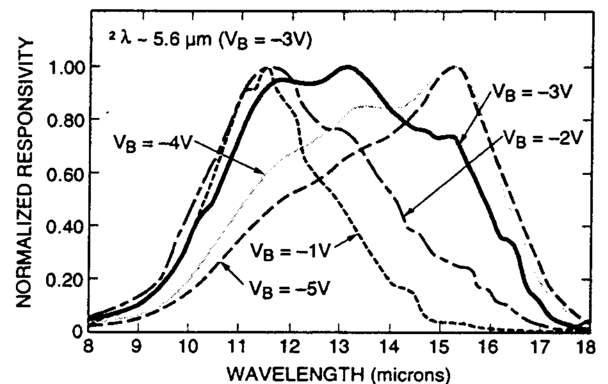


Fig. 5. Experimental measurements of the normalized responsivity spectrum of broad-band QWIP under different bias voltages.

Unlike narrow-band QWIPs, these detectors show spectral peak shifts from $\lambda$ = 11.5 μm to $\lambda$ = 15.1 μm as negative bias voltage increased from $V_B$ = -1 V to $V_B$ = -5 V ( See Fig. 5) and similar behavior ( $\lambda$ = 11.5 μm to $\lambda$ = 14.7 μm for $V_B$ = +1 V to $V_B$ = +5 V) was observed under positive bias voltages as well. This suggests that there is no substantial carrier depletion due to the applied electric field within the three-quantum-units because the direction of peak shift remains the same under both positive and negative biases. The bias dependence of absolute spectral responsivity at three different wavelengths are shown in Fig. 6. The cause of this peak shift can be explained using optical gain ($g_p$) of QWIP which is defined by [9-12] $R = (e/h\nu)\eta g_p$ where $R$ is the responsivity, $\eta$ is the absorption quantum efficiency (QE), $e$ is the electronic charge, and $h\nu$ is the photoexcitation energy. Fig. 7 shows the experimental behavior of $g_p$ vs $V_B$ for wavelengths $\lambda$ = 11.5 μm, $\lambda$ = 12.0 μm, $\lambda$ = 13.2 μm, and $\lambda$ = 15.1 μm. These curves were determined by measuring spectral responsivity and absorption of the detector. For longer wavelengths, it is required to apply a higher bias voltage to obtain reasonable none-zero values for $g_p$, while for shorter wavelengths $g_p$ starts from zero bias. This can be attributed to the behavior of transmission probability factor ( $\gamma$) in $g_p$ , i.e. $g_p \propto \gamma$ [10]. The $\gamma$ is smaller for longer wavelength transitions due to the fact that the excited states associated with longer wavelength transitions are more bound in the quantum well (See Fig. 3) compared to excited states associated with shorter wavelengths.

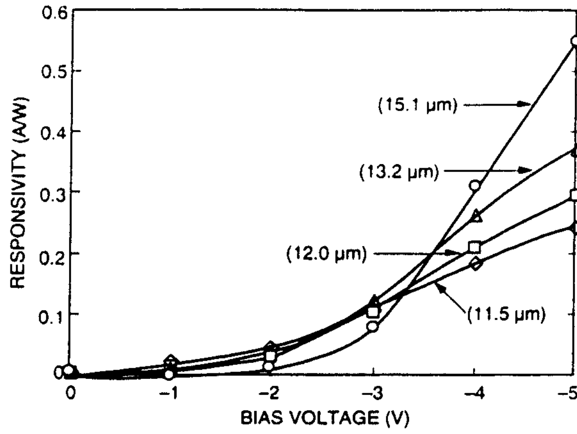


Fig. 6. The bias dependence of the absolute responsivity at wavelengths λ = 11.5 μm, λ = 12.0 μm, λ = 13.2 μm, and λ = 15.1 μm.

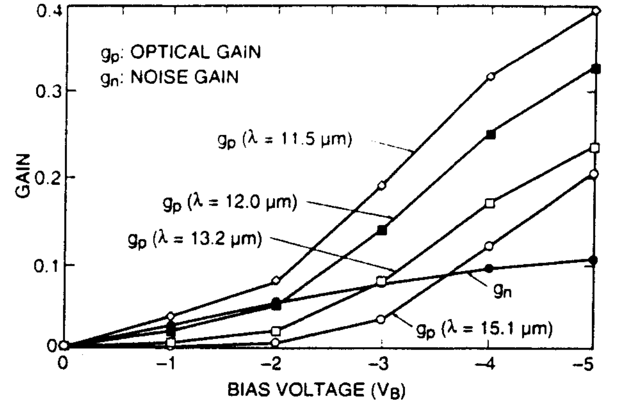


Fig. 7. Experimental behavior of optical gain($g_p$) and noise gain ($g_n$) vs $V_B$ for wavelengths λ = 11.5 μm, λ = 12.0 μm, λ = 13.2 μm, and λ = 15.1 μm.

## 4. GAIN

The dark current noise $i_n$ of the device was measured using a spectrum analyzer [4,5] at T = 55 K as a function of bias voltage. The noise gain $g_n$ can now be obtained using the g-r noise calculated based on standard noise expression:[4,5,9-12] $i_n = \sqrt{4eI_d g_n \Delta B}$ where $I_d$ is the dark current and $\Delta B$ is the band width. Combining the measurements of $i_n$ and $I_d$, experimentally determined behavior of $g_n$ vs $V_B$ is shown in Fig.7. For a typical QWIP, where the dark current is dominated by thermionic emission, $g_n$ and $g_p$ are related by the expression:[10]

$$g_p = \gamma(g_n - 1/2N) \tag{1}$$

where $N$ is the number of quantum wells in the QWIP. According to this equation, for a MQW structure with high $N$, $g_p < g_n$ for bound-bound structures ( $\gamma < 1$) and $g_p \rightarrow g_n$ for bound to continuum structures ($\gamma \rightarrow 1$).An assumption made in the derivations of $g_p$ and $g_n$ in this expression is that, both photocurrent and dark current electrons transported in the same current path after leaving the original well, are subjected to similar capture probabilities in each well [10-12]. This assumption holds very well for MQW structures with thick barriers separating quantum wells where the dark current is dominated by thermionic emission. The present structure consists of 99 quantum wells, and 66 of those are separated by thin barriers where tunneling dominates the dark current. As shown in Fig. 3, dark current electrons tunnel through thin barriers and then thermally excite ( or thermally assisted tunnel ) across thick barriers. Although the final dark current of this device structure is dominated by thermionic emission over the thick barrier, dark current electrons and photocurrent electrons transported in two different paths result in two different capture probabilities associated with each process [10-12]. Therefore, Eq. (1) does not hold for this structure and the expression for noise gain, $g_n$ becomes more complicated [10-12]. One can analyze noise gain and optical gain expressions ($g_n = (1-p_c/2)/Np_c$ and $g_p = \gamma(1-p_c)/Np_c$ where $p_c$ is the capture probability of electrons by the next period of the MQW[10] ), for a less complicated case where the dark current is completely dominated by tunneling. In this case, all dark current electrons tunnel via lower energy ground states are captured by the next well (i.e. $p_c \rightarrow 1$), while most of the photoecxcited electrons escape via higher energy excited states (i.e. $p_c \rightarrow 0$). Thus, $g_n \rightarrow 1/2N$ and $g_p \rightarrow \gamma/Np_c$ [10,11] expressions can be different according to the energy of the carriers involved in each process. At higher operating biases, where $\gamma \rightarrow 1$, when the tunneling is present, optical gain can be higher than noise gain ($g_p > g_n$) in MQW structures. Within this context, behavior of $g_p$ and $g_n$ shown in Fig. 6, can be understood because in the present device, dark current electrons transport via tunneling and thermal excitation.

Using experimental measurements of noise and responsivity, one can now calculate specific detectivity[4,5] $D^*$ form $D^* = R\sqrt{A\Delta f} / i_n$, where $A$ is area of the detector. Calculated D* value for the present device at $\lambda$ = 15.2 μm, T = 55 K, and $V_B$ = 4 V is 1 x $10^{10}$ cm$\sqrt{Hz}$/W. Even with broader response, this $D^*$ is comparable to previously reported $D^*$ of QWIPs with narrow spectral response [6-8]. Further work on improving the gain ratio $g_p/g_n$ is expected to significantly improve the $D^*$ and the operating temperature of the device.

Unlike the responsivity spectrums of intrinsic infrared detectors, the responsivity spectrums of QWIPs are much narrower and sharper due to their resonance intersubband absorption.[1,2] The normalized responsivity spectra $R(\lambda)$ are given in Fig. 3, where we see that the *bound* and *quasibound* excited state QWIPs are much narrower $\Delta\lambda/\lambda$ ~ 10% than the *continuum* QWIPs $\Delta\lambda/\lambda$ = 24 %. This is due to the fact that, when the excited state is placed in the continuum band above the barrier, the energy width associated with the state becomes wide. Spectral band width of these QWIPs can be further increased by increasing the carrier density and by slightly varying the parameters of each well in the multi-quantum well structure[7] (See Figure 4). This device structure involves several repeated layers of three different GaAs/$Al_xGa_{1-x}As$ quantum wells separated thick $Al_xGa_{1-x}As$ barriers. The thickness of the GaAs layer of these three quantum wells are designed to respond at peak wavelengths 13.5 μm, 14.3 μm and 15.5 μm respectively. These measurements show broadening of the spectral response up to $\Delta\lambda$ ~ 6 μm, (i.e. the full width at the half maximum from 13.2 - 16.6 μm). This broadening $\Delta\lambda/\lambda_p$ ~ 46% is more than a 400 % increase compared to a typical bound-to-quasibound QWIP. This band width can be tuned to a desired value by varying the structure parameters.[7]

The absolute peak responsivity ($R_p$) can be written in terms of quantum efficiency ($\eta$) and photoconductive gain (g) as $R_p = (e/h\nu)\eta g$. The bias dependence of $R_p$ is shown in Fig. 5. Note that at low bias the responsivity is nearly linearly dependent on bias and it saturates at high bias. This saturation occurs due to the saturation of carrier drift velocity. The responsivity of more *bound-to-bound* samples has a significantly different shape. The responsivity does not start out linearly with bias, but is in fact zero for finite bias. That is, there is a zero bias offset of more than 1 V, due to the necessity of field assisted tunneling for the photoexcited carrier to escape from the well.

At low operating bias voltages, responsivity spectrum of bound-to-bound QWIPs show additional peaks due to resonance energy levels of potential barriers (See Figure 6). The absorption between ground state and barrier resonance levels are much smaller than that of the ground and first excited state. The escape probability of the photoexcited electrons at the bounded first excited state is much smaller under lower operating bias voltages. As the bias increases, the escape probability of the photoexcited electrons at the excited state (bounded to the well) also increases. Thus the peak associated with the bound to excited transition becomes dominant in the spectrum. Also, due to the same reason, bound-to-continuum QWIPs do not show any responsivity peaks associated with barrier resonances.

In summary, we have demonstrated a broad-band GaAs/AlGaAs QWIP which is sensitive over 10 - 16 μm spectral range showing a broadening of $\Delta\lambda/\lambda_p$ ~ 42% at the half maximum, about a 400% increase compared to a typical bound-to-quasibound QWIP. In this device structure, which is different from typical QWIPs, we have observed and explained the physics of two different gain mechanisms associated with the photo-electrons and the dark-electrons.

## 5. ACKNOWLEDGEMENT

The research described here was performed by the Center for Space Microelectronics Technology, Jet Propulsion Laboratory, California Institute of Technology, and was jointly sponsored by the Ballistic Missile Defense Organization/ Innovative Science & Technology Office, and the National Aeronautics and Space Administration, Office of Space Science.

## 6. REFERENCE:


[1] S. D. Gunapala, J. S. Park, G. Sarusi, T. L. Lin, J. K. Liu, P. D. Maker, R. E. Muller, C. A. Shott, T. Holter, and B. F. Levine, IEEE Trans. Ele. Devices, vol. 44, 45-50 (1997).

[2] S. D. Gunapala, J. K. Liu, J. S. Park, M. Sundaram, C. A. Shott, T. Holter, T. L. Lin, S. T. Massie, P. D. Maker, R. E. Muller, and G. Sarusi, IEEE Trans. Elec. Devices, vol. 44, 51-57 (1997).

[3] S. D. Gunapala, S. V. Bandara, J. K. Liu, W. Hong, M. Sundaram, R. Carralejo, C. A. Shott, P. D. Maker, and R. E. Muller, SPIE Proceeings, V 3061, 124 (1997).

[4] S. D. Gunapala and K. M. S. V. Bandara, Physics of Thin Films, edited by M. H. Francombe, and J. L. Vossen, Vol. 21, pp. 113-237, Academic Press, NY, 1995.

[5] B. F. Levine, J. Appl. Phys. **74**, R1 (1993).

[6] A. Zussman, B. F. Levine, J. M. Kuo, and J. de Jong, J. Appl. Phys. **70**, 5101 (1991).

[7] B. F. Levine, A. Zussman, J. M. Kuo, and J. de Jong, J. Appl. Phys. **71**, 5130 (1992).

[8] G. Sarusi, S. D. Gunapala, J. S. Park, and B. F. Levine, J. Appl. Phys. **76**, 6001 (1994).

[9] B. F. Levine, A. Zussman, S. D. Gunapala, M. T. Asom, J. M. Kuo, and W. S. Hobson, J. Appl. Phys. **72**, 4429 (1992).

[10] K. K. Choi, J. Appl. Phys. **80**, 1257 (1996).

[11] H. C. Liu, Appl. Phys. Lett. **61**, 2703 (1992).

[12] W. A. Beck, Appl. Phys. Lett. **63**, 3589 (1993).